

A Chemometrics-driven Strategy for the Bioactivity Evaluation of Complex Multicomponent Systems and the Effective Selection of Bioactivity-predictive Chemical Combinations

Yoshinori Fujimura^{1,#,*}, Chihiro Kawano^{1,#}, Ayaka Maeda-Murayama¹, Asako Nakamura¹, Akiko Koike-Miki¹, Daichi Yukihiro¹, Eisuke Hayakawa², Takanori Ishii¹, Hirofumi Tachibana^{1,3}, Hiroyuki Wariishi^{1,3,4}, and Daisuke Miura^{1,*}

¹Innovation Center for Medical Redox Navigation, Kyushu University, 3-1-1 Maidashi, Higashi-ku, Fukuoka 812-8582, Japan; ²Okinawa Institute of Science and Technology Graduate University, 1919-1 Tancha, Onna-son, Kunigami-gun, Okinawa 904-0495, Japan; ³Faculty of Agriculture and ⁴Faculty of Arts and Science, Kyushu University, 6-10-1 Hakozaki, Higashi-ku, Fukuoka 812-8581, Japan.

#These authors equally contributed to this work.

*Correspondence and requests for materials should be addressed to Y. F. (email: fujimurayoshinori@gmail.com) or D.M. (email: daipon@agr.kyushu-u.ac.jp)

The authors declare no conflict of interest.

Contents:

Supplementary methods

LC–MS analysis

Supplementary Figures and Tables

Supplementary Figure S1. The schematic flow of the peak picking and alignment of non-targeted MALDI–MS data.

Supplementary Figure S2. Heatmap representation of the ionization of the representative phytochemicals by MALDI–MS using four matrices dissolved in MeOH solution.

Supplementary Figure S3. The representative relationship between the chemical structure and the ionization efficiency of phytochemicals.

Supplementary Figure S4. The correlation plot of the highest VIP-valued compounds at the concentration level of GTEs.

Supplementary Figure S5. The chart visualization of the observed ORAC values of GTEs using the selected combinations with the highest correlation values.

Supplementary Figure S6. The chart visualization of the observed ORAC values of GTEs using the selected combination with low correlation value.

Supplementary Figure S7. Scheme of chemometrics-driven selection of GTE bioactivity-correlated chemical combinations.

Supplementary Figure S8. Comparison of the MALDI–MS-MP system with the conventional strategy in view of 2 distinct research fields.

Supplementary Figure S9. LC–MS-MP of 21 GTEs for evaluating their quality and bioactivity.

Supplementary Figure S10. The effect of components with the highest VIP values (>1) on the construction of OPLS regression models.

Supplementary Figure S11. The evaluation of the robustness of the present MALDI–MS-MP system.

Supplementary Figure S12. Graphical representation of MALDI–MS-MP system for the bioactivity evaluation of diverse bioactive sample panels representing multicomponent systems and the effective selection of bioactivity-predictive chemical combinations.

Supplementary Table S1. The ionization rates of the representative phytochemicals for MALDI matrix screening.

Supplementary Table S2. MALDI–MS datasets of 21 GTEs for multivariate statistical analyses.

Supplementary Table S3. The top-40 VIP-valued components highly contributing to the construction of OPLS regression model and their correlations with ORAC values.

Supplementary Table S4. Combinations of multiple components with the highest VIP values (>1) and their correlation values using three abundance measures.

Supplementary Table S5. LC–MS datasets of 21 GTEs for multivariate statistical analyses.

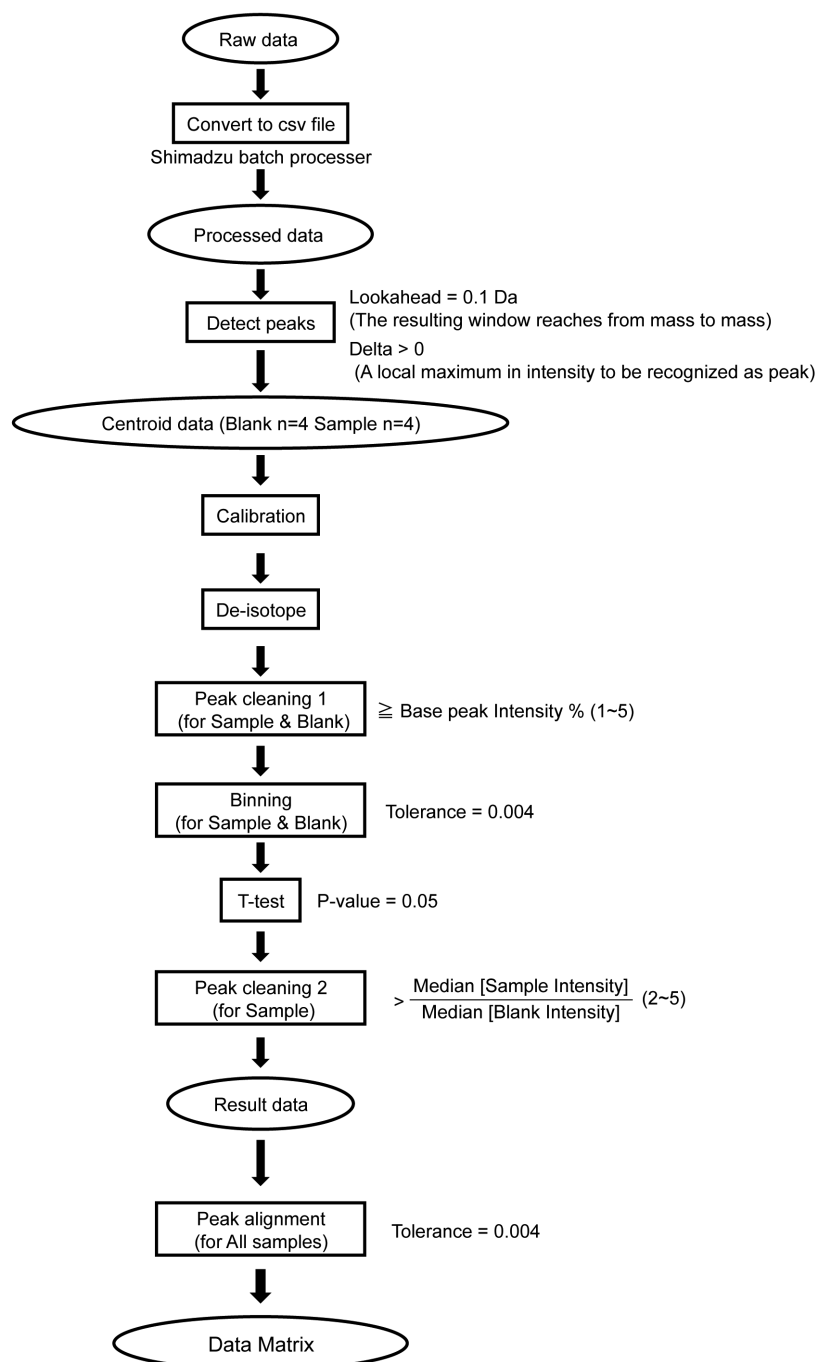
Supplementary Table S6. Selected peaks with the highest VIP values (>1) contributing to the construction of OPLS regression models in LC–MS datasets.

Supplementary Table S7. Selected peaks with the highest VIP values (>1) contributing to the construction of the polyphenol-predictive OPLS regression model in MALDI–MS datasets.

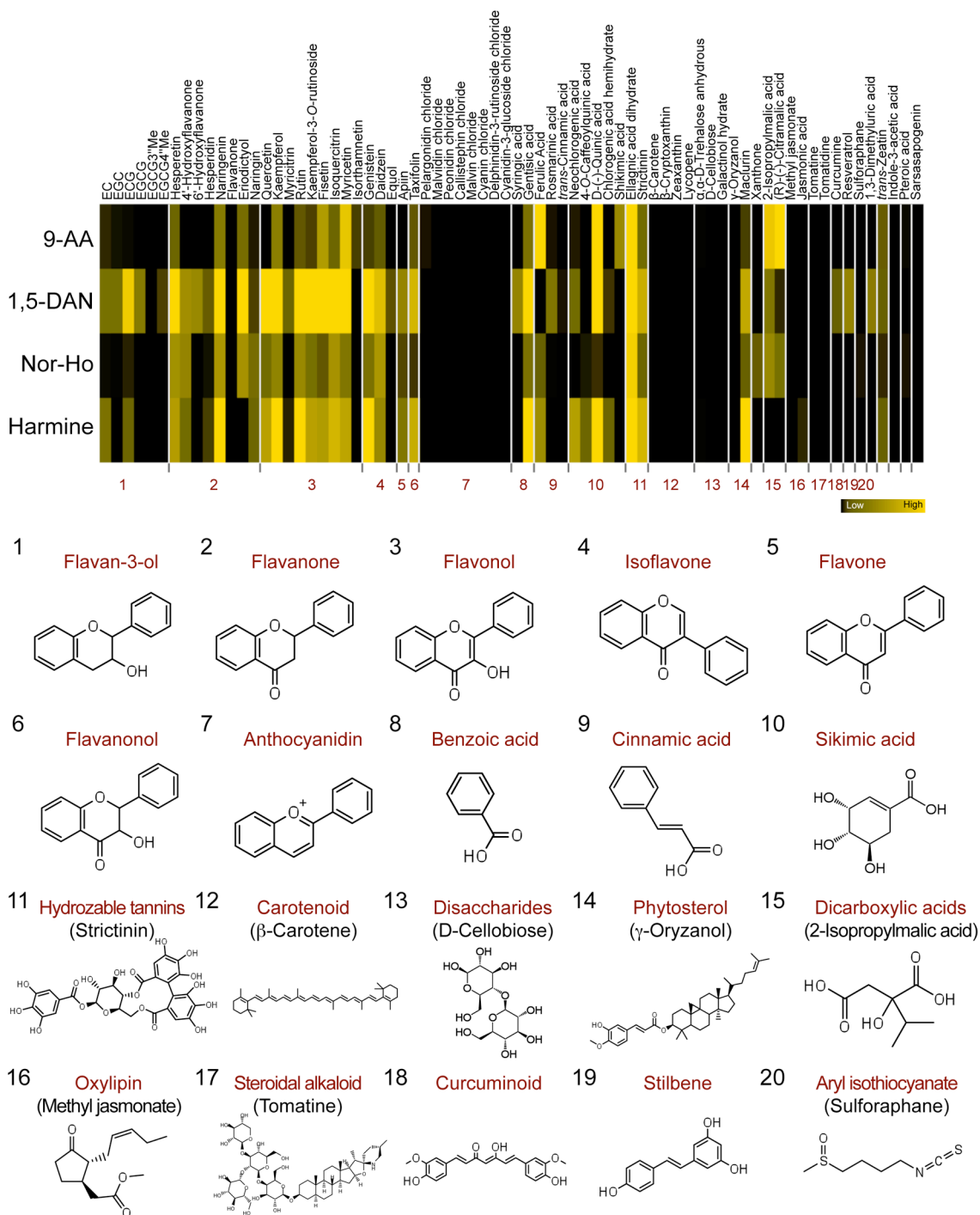
Supplementary methods

LC–MS analysis. All GTEs were subjected to LC–MS analysis using a LCMS-IT-TOF instrument (Shimadzu, Kyoto, Japan). The instrument was fitted with a Luna C18(2) column (250 mm × 1.0 mm, 5 μm particle size, Phenomenex, Torrance, CA) maintained at 40°C. The mobile phase solvents were 0.1% aqueous formic acid (solvent A) and methanol (solvent B). Solvent B was 5% for 2.0 min, increased linearly from 5% to 60% over 6.0 min, and further increased from 60% to 100% at 13.0 min, and 100% holding for 4.5 min. Flow rate was constant (0.1 mL/min). The MS instrument was operated using an ESI source in both positive and negative ionization modes with survey scans acquired from m/z 100 to 700. Ionization parameters were as follows: capillary voltage, 4.5 kV and –3.5 kV; nebulizer gas flow, 1.5 L/min; CDL temperature, 250°C; heat block temperature, 250°C. Individual GTEs were diluted 1:50 in distilled water, and then 2.5 μM 4 hydroxybenzophenone was added as an internal standard. Samples were filtered through a 0.22-μm PTFE filter, and 5 μL was injected onto the column for each run.

Supplementary Figures and Tables

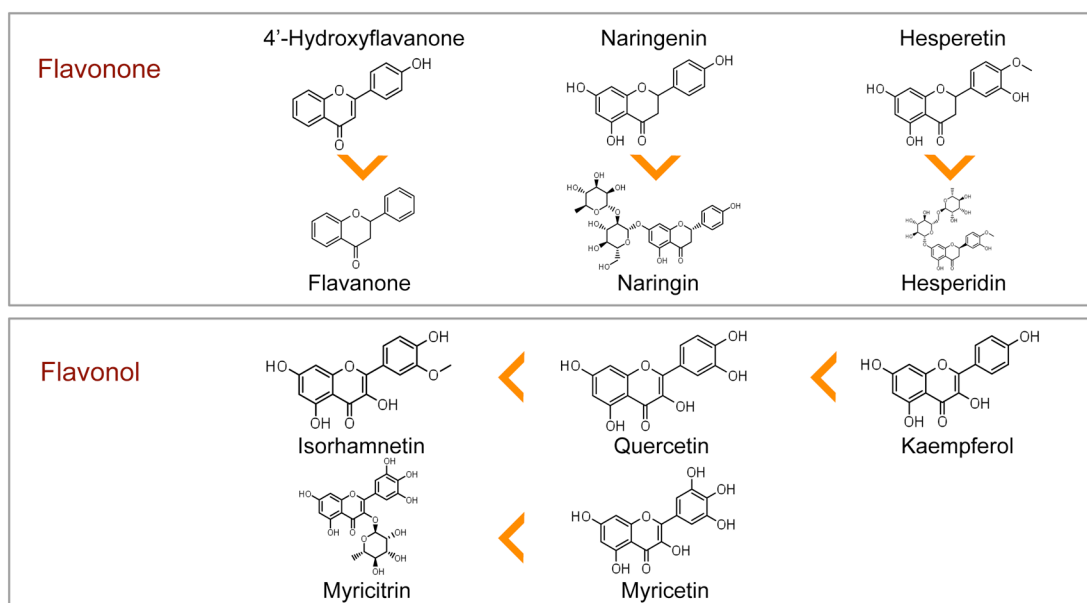


Supplementary Figure S1. The schematic flow of the peak picking and alignment of non-targeted MALDI-MS data.

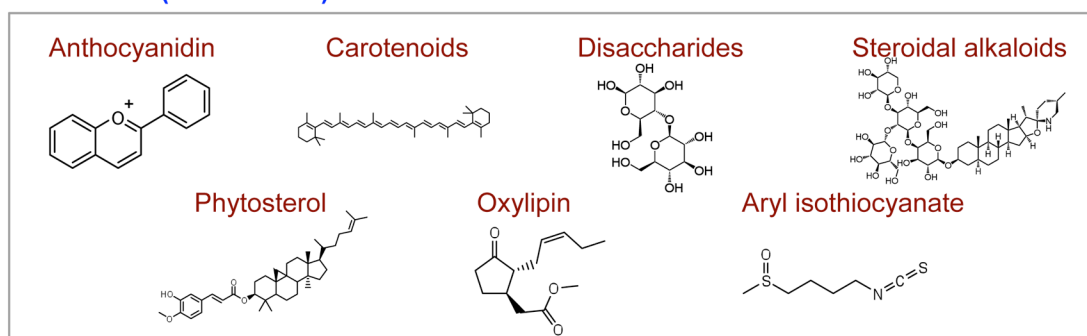


Supplementary Figure S2. Heatmap representation of the ionization of the representative phytochemicals by MALDI-MS using four matrices dissolved in MeOH solution. Heatmap analysis showing the different ionization rates of the 72 phytochemicals by the 4 matrices dissolved in 100% MeOH solution. In addition, 20 representative chemical structures of phytochemicals are illustrated.

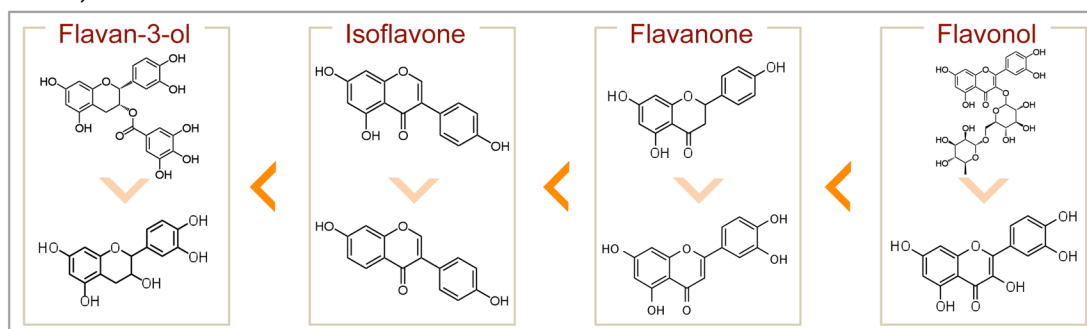
A Detection (High)



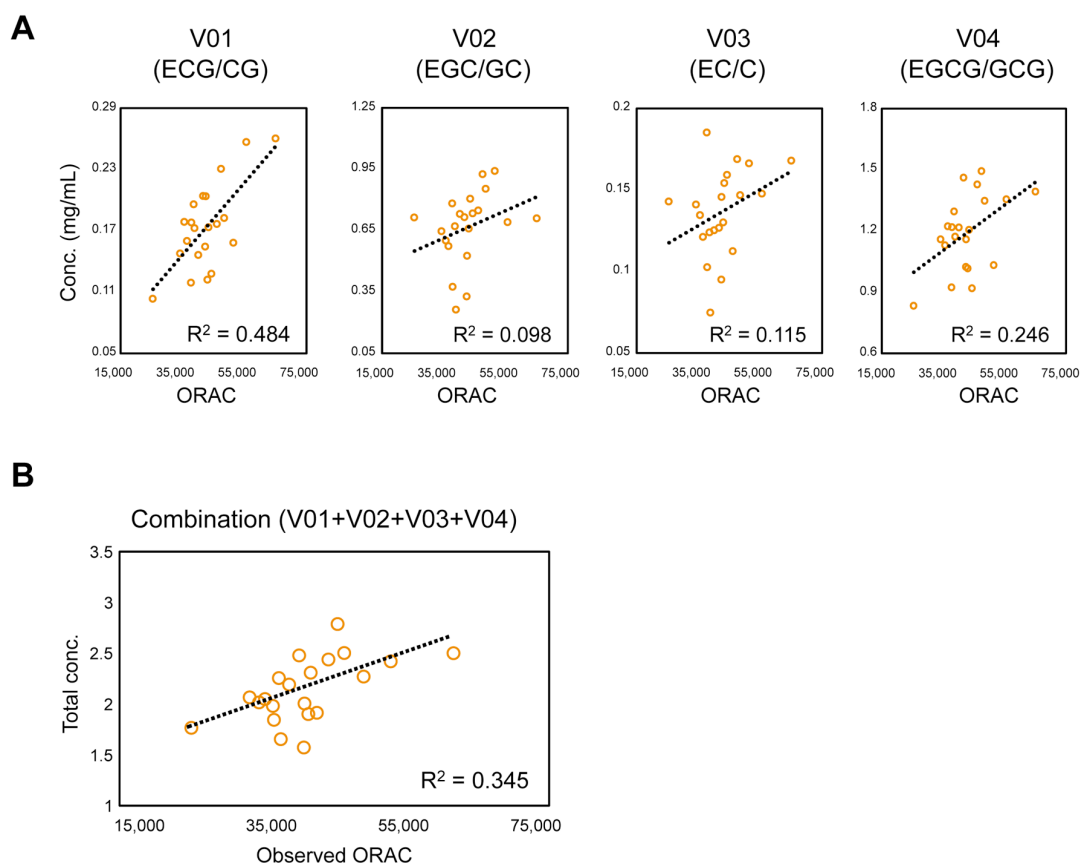
Detection (Zero or Low)



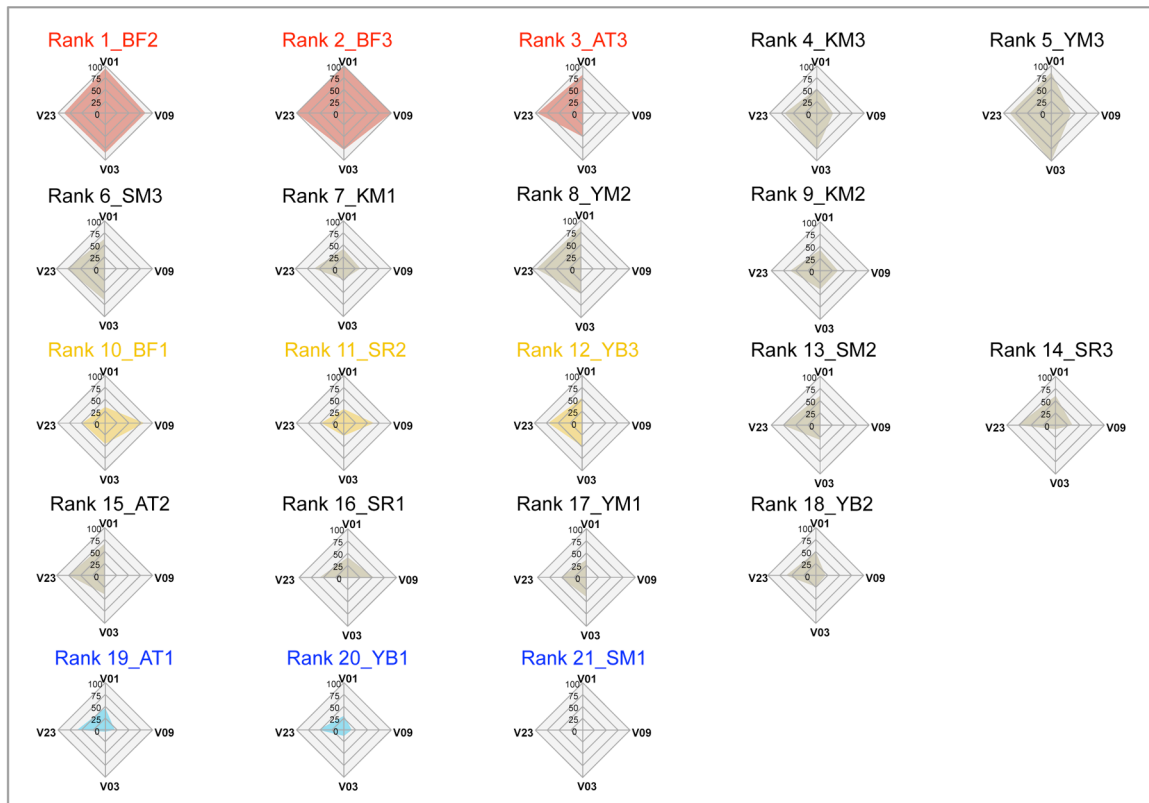
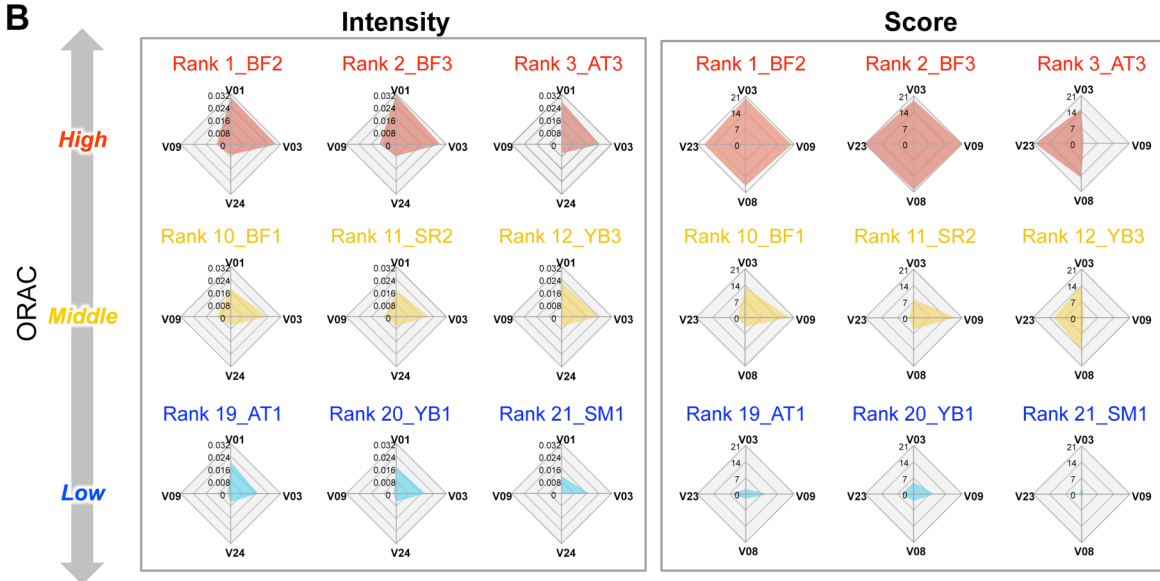
B 1,5-DAN



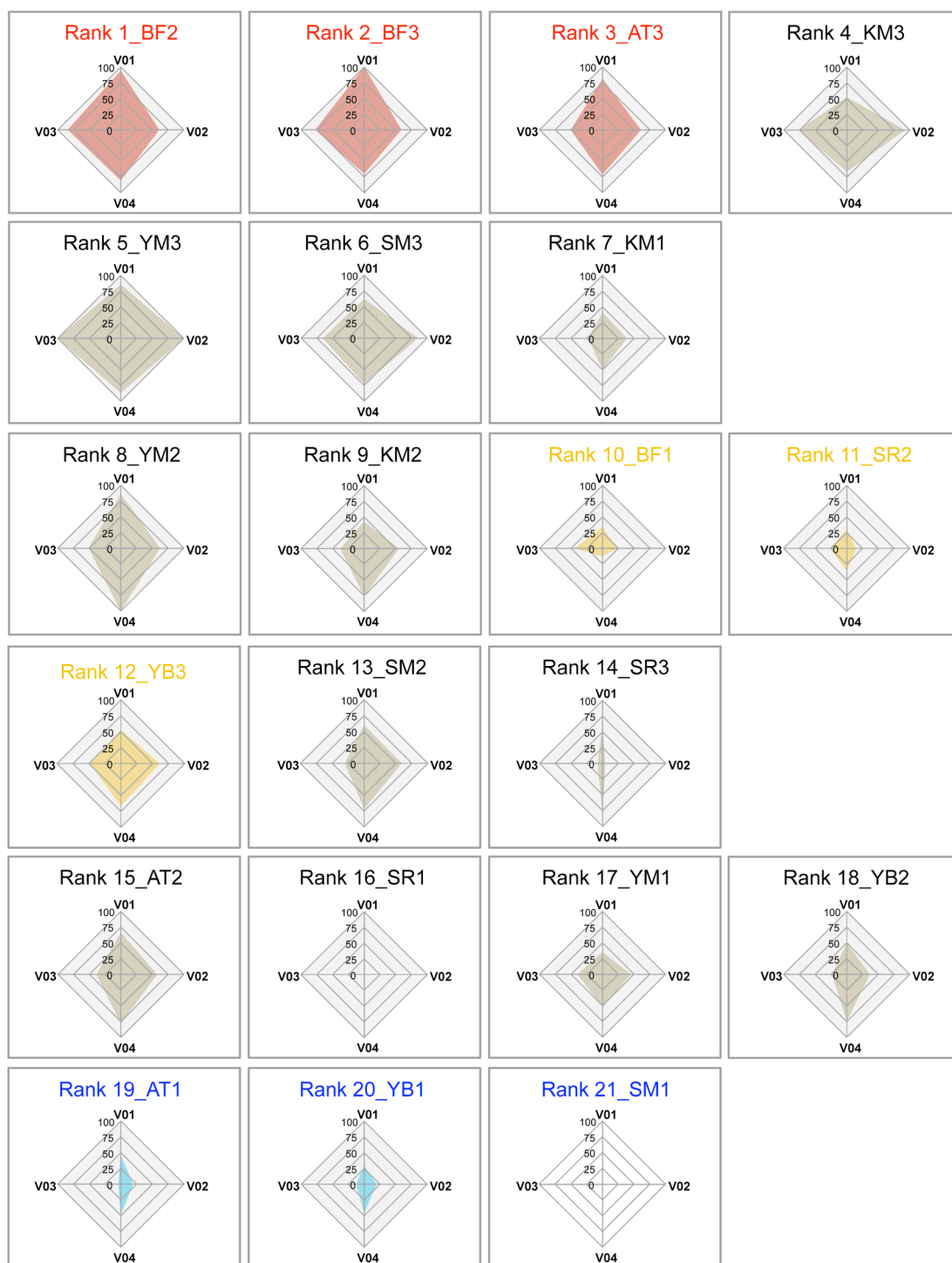
Supplementary Figure S3. The representative relationship between the chemical structure and the ionization efficiency of phytochemicals. Among the phytochemicals with different detectability, their representative relationships with the ionization efficiency are shown under conditions observed in (A) four matrices or (B) 1,5-DAN alone. The ionization efficacy of the phytochemicals is partially dependent on the position and the number of glycosylation, methylation, and hydroxylation.



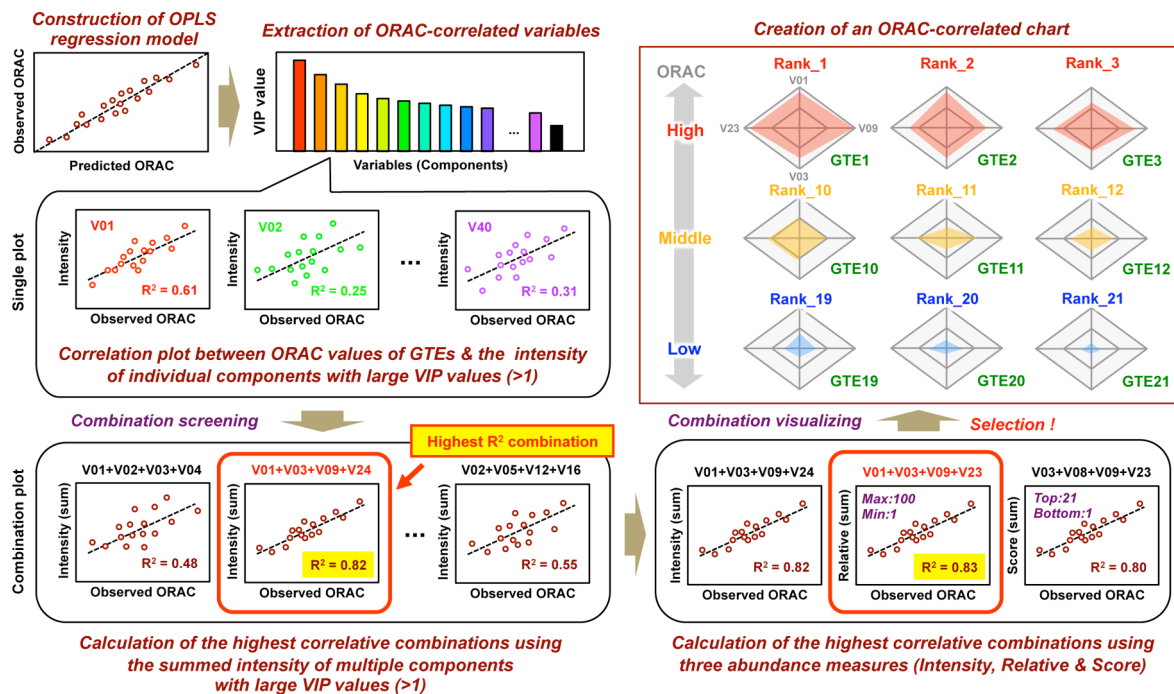
Supplementary Figure S4. The correlation plot of the highest VIP-valued compounds at the concentration level of GTEs. (A) Correlations between ORAC and the concentration of each of the top-4 components with the largest VIP values (>1). **(B)** Correlations between ORAC and the summed concentrations of the top-4-VIP components.

A**Relative****B**

Supplementary Figure S5. The chart visualization of the observed ORAC values of GTEs using the selected combinations with the highest correlation values. (A) Observed ORAC values of GTEs visualized as radar charts using information from the 4 selected components (V01+V03+V09+V23). Charts for all GTEs are shown. (B) A representative section of the charts for nine GTEs is also illustrated using the Intensity data of the combination (V01+V03+V09+V24) or the Score data of the combination (V03+V08+V09+V23)



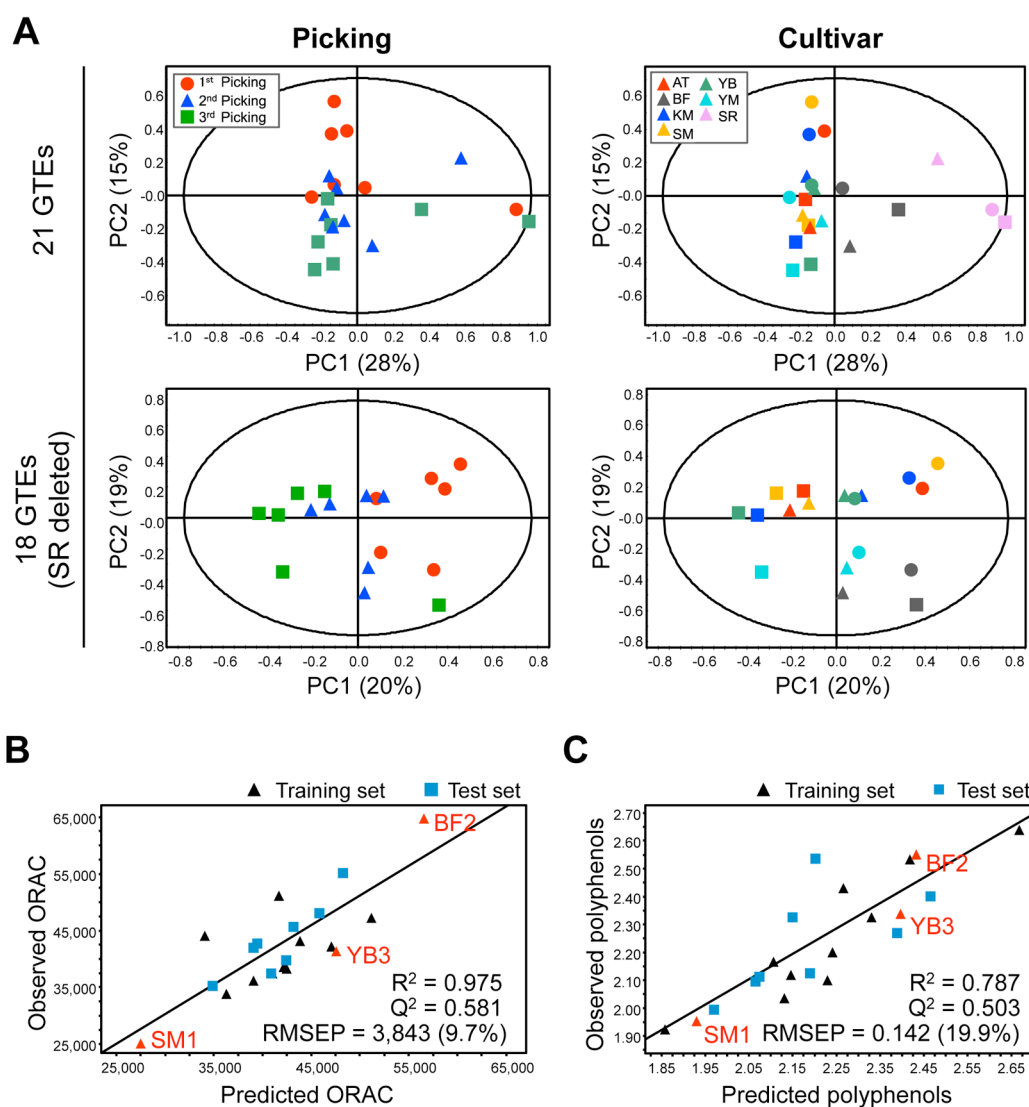
Supplementary Figure S6. The chart visualization of the observed ORAC values of GTEs using the selected combination with low correlation value. Observed ORAC values of GTEs visualized as radar charts using information from the 4 selected components (V01+V02+V03+V04) with low correlation value. Charts for all GTEs are shown.



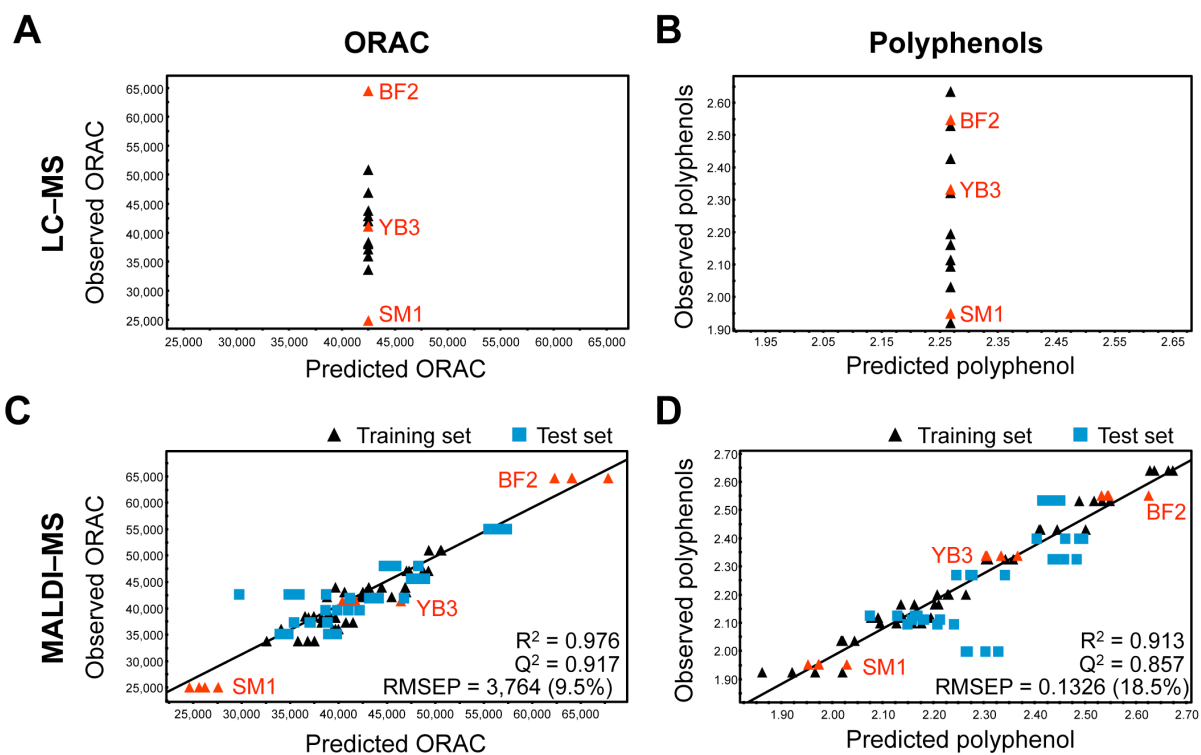
Supplementary Figure S7. Scheme of chemometrics-driven selection of GTE bioactivity-correlated chemical combinations.

	<i>In View of Pharmaceutical, Nutraceutical, & Food Functionality Researches</i>		<i>In View of Metabolomics Research</i>	
	Conventional strategy	Novel strategy (MALDI-MS-MP)	Conventional strategy (LC-MS-MP or GC-MS-MP)	
Evaluation target	Single	Multiple		
Evaluation unit	Absolute quantity	Compositional balance		
Narrowing candidate components contributed to bioactivity	Multiple steps	One step		
Decision process of combination of multiple components	Hypothesis or experiment-driven	Hypothesis-generating or data-driven		
Bioassay validation (Frequency; labor-intensive)	High	Low		
		○	×	Direct analysis of crude sample
		◎	△	Rapid & high-throughput
		◎	△	Extensibility of sample number (>1,000)
		○	○	Theoretical presentation of combination for bioactivity
		△	◎	Detective performance of small molecules

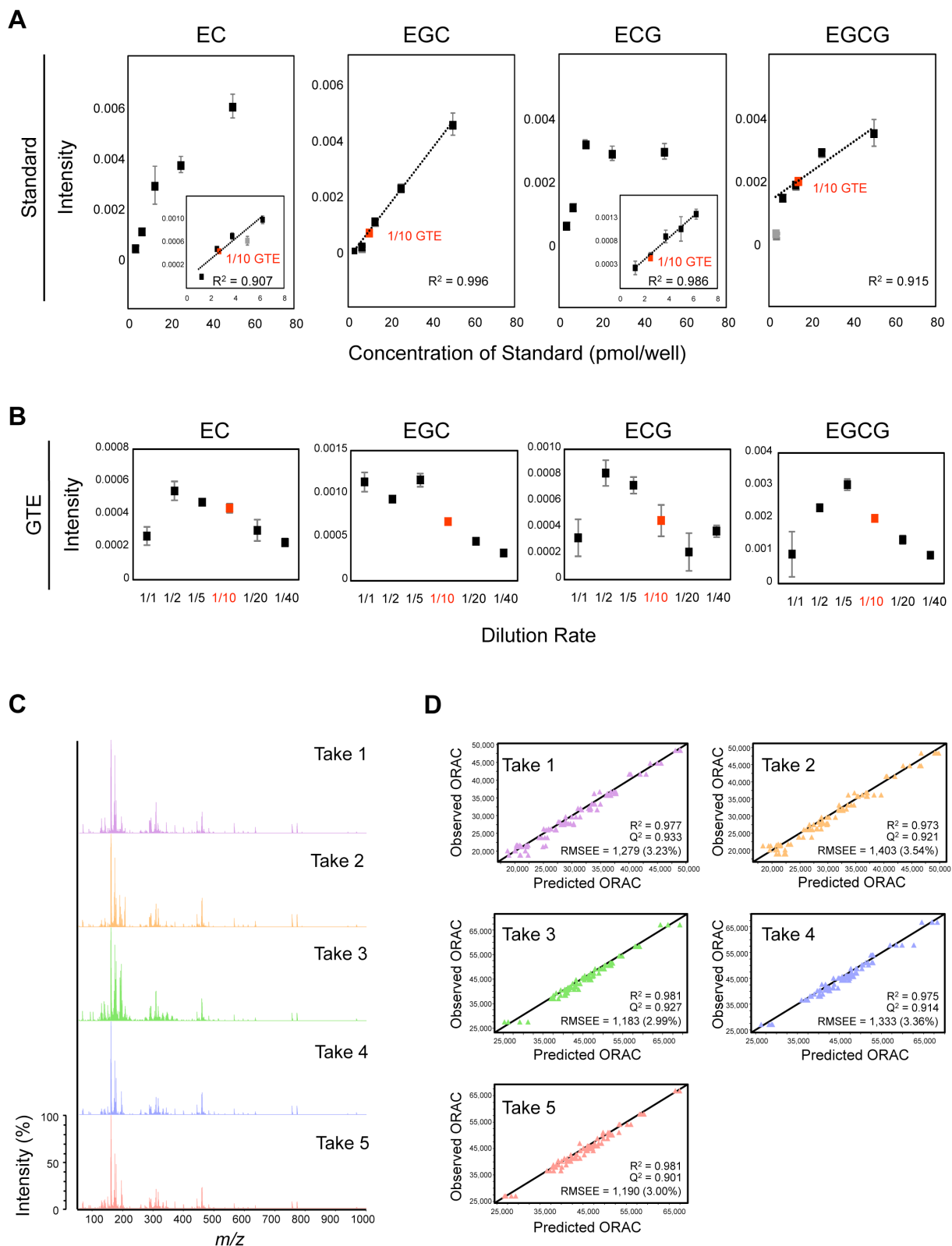
Supplementary Figure S8. Comparison of the MALDI-MS-MP system with the conventional strategy in view of 2 distinct research fields.



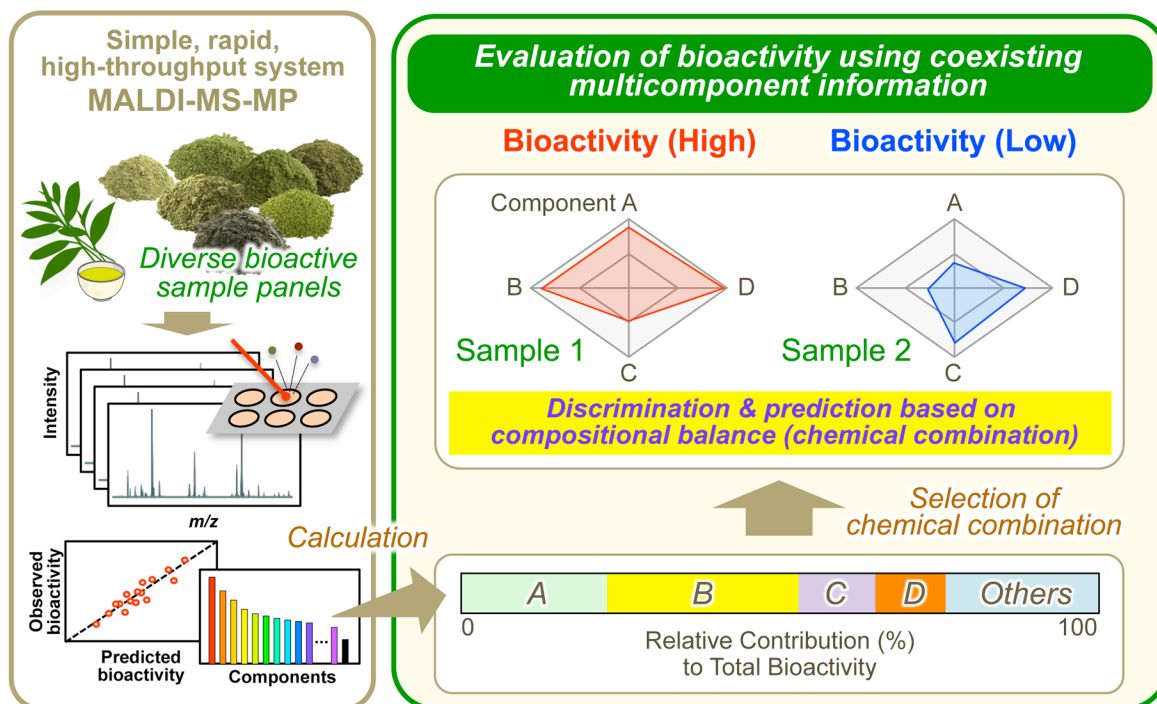
Supplementary Figure S9. LC–MS–MP of 21 GTEs for evaluating their quality and bioactivity. (A) PCA score plot of LC–MS datasets of 21 GTEs showing different clusters of MS profiles, based on the attributes of picking seasons and cultivars. (B) Models for predicting (B) ORAC or (C) total polyphenol content were calculated from the LC–MS datasets of 21 GTEs, including 13 training (black triangles) and 8 test (blue squares) sets.



Supplementary Figure S10. The effect of components with the highest VIP values (>1) on the construction of OPLS regression models. Models for predicting ORAC (**A**, **C**) or total polyphenol content (**B**, **D**) were calculated from the LC-MS (**A**, **B**) or MALDI-MS (**C**, **D**) datasets of 21 GTEs, including 13 training (black triangles) and 8 test (blue squares) sets. These models were constructed using datasets excluding components with the highest VIP values (>1).



Supplementary Figure S11. The evaluation of the robustness of the present MALDI-MS-MP system. (A) The calibration curve from the representative GTE components (EGCG, EGC, ECG, and EC at the standard level) in MALDI-MS system. In EC and EGCG, the coefficient of determination (R^2) was calculated using datasets excluding the value of grey square symbol. Red square symbol indicates the data corresponding to 1/10 GTE sample. (B) Plots of these four compounds detected in a dilution series of the representative GTE (YB1). Data are shown as mean \pm SD ($n=3-5$). (C) Verification of the repeatability of MS data acquired on a different day using the representative GTE (YB1). (D) OPLS regression models using such MS datasets.



Supplementary Figure S12. Graphical representation of MALDI–MS–MP system for the bioactivity evaluation of diverse bioactive sample panels representing multicomponent systems and the effective selection of bioactivity-predictive chemical combinations.

Supplementary Table S1. The ionization rates of the representative phytochemicals for MALDI matrix screening.

	m/z		Acetone				MeOH			
	Theoretical	Observed [M-H]	9AA	1,5-DAN	Nor-Ho	Harmine	9AA	1,5-DAN	Nor-Ho	Harmine
EC	290.08	289.07	0.0016	0.0045	0.0006	0.0062	0.0011	0.0070	0.0005	0.0072
EGC	306.08	305.15	0.0003	0.0083	0.0001	0.0022	0.0005	0.0067	0.0003	0
ECG	442.09	441.17	0.0018	0.0123	0.0048	0.0058	0.0004	0.0282	0.0010	0.0046
EGCG	458.08	457.13	0.0002	0.0066	0.0009	0.0007	0	0.0092	0.0001	0
EGCG3*Me	472.10	471.12	0	0.0034	0.0002	0.0002	0	0	0.0001	0
EGCG4*Me	472.10	471.03	0	0.0033	0.0008	0.0004	0	0.0019	0.0001	0
Hesperetin	302.08	301.05	0.0095	0.0574	0.0154	0.0245	0.0049	0.0559	0.0147	0.0174
4'-Hydroxyflavanone	240.08	239.11	0.0026	0.0182	0.0086	0.0125	0	0.0144	0.0125	0.0060
6'-Hydroxyflavanone	240.08	239.07	0	0.0157	0.0001	0.0007	0	0.0127	0	0
Hesperidin	610.19	609.28	0.0008	0.0039	0.0005	0.0028	0	0.0036	0.0006	0.0018
Naringenin	272.07	271.09	0.0170	0.0524	0.0450	0.0444	0.0092	0.0683	0.0164	0.0582
Flavanone	224.08	223.10	0.0008	0.0010	0.0001	0	0	0	0.0001	0
Eriodictyol	288.07	287.12	0.0151	0.0500	0.0119	0.0658	0.0065	0.0520	0.0151	0
Naringin	580.18	579.23	0.0017	0.0059	0.0056	0.0033	0.0009	0.0020	0.0062	0.0049
Quercetin	302.04	301.08	0.0146	0.0364	0.0143	0.0245	0	0.0687	0.0054	0.0182
Kaempferol	286.05	285.09	0.0192	0.0559	0.0251	0.0399	0.0103	0.0538	0.0116	0.0344
Myricitrin	464.10	463.19	0.0012	0.0034	0.0004	0.0052	0	0.0045	0.0002	0.0009
Rutin	610.15	609.23	0.0112	0.0702	0.0189	0.0316	0.0030	0.0486	0.0126	0.0302
Kaempferol-3-O-rutinoside	594.16	593.23	0.0075	0.0410	0.0162	0.0183	0.0020	0.0328	0.0067	0.0185
Fisetin	286.05	285.10	0.0294	0.0339	0.0086	0.0183	0.0170	0.0372	0.0031	0.0168
Isoquercitrin	464.10	463.20	0.0165	0.0276	0.0179	0.0190	0.0048	0.0438	0.0151	0.0231
Myricetin	318.04	317.09	0.0275	0.0474	0.0179	0.0179	0.0264	0.0511	0.0088	0.0192
Isorhamnetin	316.06	315.08	0.0017	0	0	0	0.0018	0	0	0
Genistein	270.05	269.11	0.0037	0.0488	0.0145	0.0221	0.0019	0.0448	0.0071	0.0427
Daidzein	254.06	253.10	0.0035	0.0289	0.0148	0.0112	0.0034	0.0247	0.0159	0.0125
Equol	242.09	241.08	0	0.0080	0	0	0	0.0026	0	0.0001
Apiin	564.15	563.27	0.0023	0.0089	0.0076	0.0043	0	0.0120	0.0022	0.0085
Taxifolin	304.06	303.11	0.0074	0.0149	0.0085	0.0209	0.0031	0.0227	0.0015	0.0210
Pelargonidin chloride	306.03	305.04	0.0006	0	0	0	0.0007	0	0	0
Malvidin chloride	366.05	365.06	0	0	0	0.0002	0	0	0	0
Peonidin chloride	336.04	335.11	0.0004	0	0	0.0002	0	0	0	0
Callistephin chloride	468.08	-	0	0	0	0	0	0	0	0
Malvin chloride	690.16	-	0	0	0	0	0	0	0	0
Cyanin chloride	646.13	-	0	0	0	0	0	0	0	0
Delphinidin-3-rutinoside chloride	646.13	-	0	0	0	0	0	0	0	0
Cyanidin-3-glucoside chloride	484.08	483.04	0.0002	0	0	0	0	0	0	0
Syringic acid	198.05	197.12	0	0.0161	0.0018	0	0	0.0123	0	0
Gentisic acid	154.03	152.94	0.0135	0.0311	0.0065	0.0565	0.0072	0.0833	0.0071	0.0522
Ferulic Acid	194.06	193.06	0.2511	0	0.0036	0.0161	0.2590	0	0.0038	0.0138
Rosmarinic acid	360.08	359.16	0.0026	0	0.0015	0.0076	0.0007	0.0081	0.0003	0
trans-Cinnamic acid	148.05	146.99	0	0.0010	0	0	0	0.0007	0	0
Neochlorogenic acid	354.10	353.12	0.0030	0.0092	0.0017	0.0164	0.0009	0.0059	0	0.0177
4-O-Caffeoylquinic acid (Chlorogenic acid)	354.10	353.13	0.0024	0.0011	0.0004	0.0123	0	0	0.0008	0.0046
D-(-)-Quinic acid	192.06	190.99	0.0857	0.0226	0.0072	0.0692	0.0581	0.0402	0.0014	0.0309
Chlorogenic acid hemihydrate	354.10	353.12	0.0022	0.0011	0.0009	0.0112	0	0.0014	0.0002	0.0047
Shikimic acid	174.06	173.04	0.0081	0	0.0034	0	0.0132	0	0	0
Ellagic acid dihydrate	302.01	301.04	0.0620	0.0431	0.0404	0.0660	0.0648	0.0471	0.0285	0.0700
Strictinin	634.08	633.14	0.0073	0.0105	0.0083	0.0217	0.0057	0.0213	0.0043	0.0231
β-Carotene	536.44	535.38	0	0.0001	0	0	0	0	0	0
β-Cryptoxanthin	552.44	-	0	0	0	0	0	0	0	0
Zeaxanthin	568.43	-	0	0	0	0	0	0	0	0
Lycopene	536.44	-	0	0	0	0	0	0	0	0
α,α-D-Trehalose anhydrous	342.12	341.07	0	0	0.0001	0	0.0003	0	0	0.0003
D-Cellobiose	342.12	341.15	0.0002	0	0	0	0	0	0	0
Galactinol hydrate	342.12	341.09	0.0002	0	0	0	0	0	0	0
γ-Oryzanol	602.44	601.33	0	0.0010	0	0.0001	0.0002	0	0	0
Maclurin	262.05	261.07	0.0050	0.0266	0.0059	0.0456	0.0018	0.0199	0.0041	0.0307
Xanthone	196.06	195.07	0	0	0.0112	0	0	0	0.0036	0
2-Isopropylmalic acid	176.07	175.03	0.0353	0.0112	0.0129	0.0717	0.0269	0.0085	0.0126	0
(R)-(-)-Citramalic acid	148.04	146.95	0.0696	0.0012	0.0154	0	0.0815	0.0011	0.0069	0
Methyl jasmonate	224.14	223.10	0.0011	0	0	0	0	0	0	0
Jasmonic acid	210.13	209.09	0.0030	0.0093	0.0004	0.0070	0	0	0	0.0011
Tomatine	1033.55	1032.49	0	0.0004	0.0002	0	0	0	0.0001	0
Tomatidine	415.35	-	0	0	0	0	0	0	0	0
Curcumine	368.13	367.08	0.0003	0	0.0001	0	0.0002	0.0037	0.0001	0
Resveratrol	228.08	227.17	0	0.0189	0.0002	0.0076	0	0.0121	0	0
Sulforaphane	177.03	175.92	0	0	0.0010	0	0	0	0.0006	0
1,3-Dimethyluric acid	196.06	195.08	0	0.0397	0	0.0611	0	0.0100	0	0
trans-Zeatin	219.11	218.17	0.0046	0.0113	0	0.0139	0.0035	0.0041	0.0012	0.0041
Indole-3-acetic acid	175.06	173.97	0	0	0	0.0005	0	0	0	0
Pteric acid	312.10	311.21	0	0	0.0014	0.0103	0.0004	0	0.0006	0
Sarsasapogenin	416.33	415.12	0	0	0	0	0	0	0	0

(continued)

Table with columns: m/z, R.T., Polarity, Name (CHAC), A11, A12, A13, BF1, BF2, BF3, KM1, KM2, KM3, SM1, SM2, SM3, SR1, SR2, SR3, YB1, YB2, YB3, YM1, YM2, YM3. The table contains a large number of rows (lines 1 to 4800) listing mass spectrometry data.

Supplementary Table S6. Selected peaks with the highest VIP values (>1) contributing to the construction of OPLS regression models in LC-MS datasets.

Variables	VIP	m/z	R.T	Polar	(Name)	AT1	AT2	AT3	BF1	BF2	BF3	KM1	KM2	KM3	SM1	SM2	SM3	SR1	SR2	SR3	YB1	YB2	YB3	YM1	YM2	YM3
					(ORAC)	36.61	51.482	42.552	65.065	55.612	44.001	43.717	48.544	25.445	40.191	46.160	37.930	42.436	38.953	34.266	36.545	41.729	37.746	43.496	47.566	
V01	6.37	441.07	8.943	-	0.03435	0.04153	0.04070	0.04440	0.04200	0.03910	0.02870	0.03040	0.03740	0.02393	0.03289	0.03600	0.03320	0.03700	0.03610	0.03320	0.03700	0.04040	0.03070	0.03380	0.03800	0.04040
V02	6.12	457.07	8.817	-	0.10863	0.13601	0.12600	0.12700	0.13200	0.13030	0.11000	0.11800	0.13200	0.09222	0.12879	0.14100	0.10600	0.10078	0.10800	0.11900	0.13500	0.15100	0.11200	0.12100	0.12100	0.13900
V03	4.76	795.11	2.169	-	0.02335	0.01038	0.05655	0.02800	0.01323	0.00665	0.02470	0.01600	0.00634	0.02769	0.01687	0.00914	0.01060	0.01285	0.01050	0.02370	0.01635	0.00553	0.02540	0.01600	0.01678	
V04	4.52	303.06	10.533	+	0.10869	0.04191	0.05430	0.03130	0.02026	0.02780	0.00854	0.02890	0.00827	0.05213	0.00146	0.00307	0.00006	0.04873	0.04024	0.00000	0.00784	0.03100	0.00784	0.03100	0.01330	0.01330
V05	4.10	671.81	18.04	+	0.01614	0.00541	0.00360	0.00729	0.02910	0.03200	0.00536	0.00420	0.00938	0.00420	0.03829	0.01760	0.00938	0.00479	0.03380	0.00129	0.03130	0.03410	0.01630	0.01630	0.00882	0.00390
V06	3.71	523.14	11.193	-	0.00000	0.00000	0.00000	0.00988	0.01010	0.00667	0.00000	0.00001	0.00001	0.00000	0.00000	0.00000	0.00000	0.00000	0.00000	0.00000	0.00000	0.00000	0.00000	0.00000	0.00000	
V07	3.57	445.92	8.654	-	0.00007	0.01610	0.01090	0.01330	0.01400	0.01230	0.00756	0.00960	0.00961	0.00020	0.00020	0.00020	0.01050	0.00963	0.01010	0.00075	0.00968	0.01140	0.00784	0.00604	0.01010	
V08	3.46	471.08	9.388	-	0.00016	0.00027	0.00000	0.01010	0.00883	0.00854	0.00242	0.00282	0.00451	0.00002	0.00004	0.00002	0.00534	0.00613	0.00227	0.00000	0.00024	0.00064	0.00017	0.00238	0.00394	
V09	3.26	531.14	11.069	-	0.00000	0.00000	0.00000	0.00748	0.01030	0.01320	0.00000	0.00000	0.00000	0.00000	0.00000	0.00000	0.00000	0.00000	0.00000	0.00000	0.00000	0.00000	0.00000	0.00000		
V10	3.12	205.15	10.431	-	0.01643	0.01673	0.01540	0.01060	0.01220	0.00793	0.02240	0.01870	0.01440	0.01904	0.01060	0.01630	0.01650	0.01155	0.00850	0.02308	0.02210	0.01680	0.01680	0.01680	0.01680	
V11	3.00	337.16	2.346	+	0.00194	0.00201	0.00184	0.00287	0.00049	0.01518	0.00183	0.00522	0.00061	0.00769	0.00254	0.01023	0.01016	0.00194	0.00092	0.00183	0.01116	0.00506	0.00506	0.00076	0.00218	
V12	2.95	589.16	11.082	-	0.00000	0.00000	0.00000	0.00447	0.00579	0.00498	0.00000	0.00000	0.00000	0.00000	0.00000	0.00000	0.00000	0.00000	0.00000	0.00000	0.00000	0.00000	0.00000	0.00000		
V13	2.79	523.84	11.116	-	0.00000	0.00000	0.00000	0.00532	0.00563	0.00373	0.00000	0.00000	0.00000	0.00000	0.00000	0.00000	0.00000	0.00000	0.00000	0.00000	0.00000	0.00000	0.00000			
V14	2.68	177.12	10.611	-	0.00220	0.00454	0.00666	0.00223	0.00445	0.00446	0.00000	0.00000	0.00000	0.00000	0.00000	0.00000	0.00000	0.00000	0.00000	0.00000	0.00000	0.00000	0.00000			
V15	2.75	387.11	1.833	-	0.00877	0.00555	0.00733	0.00561	0.00289	0.00516	0.00697	0.00503	0.00475	0.00509	0.00609	0.00465	0.00369	0.00447	0.00485	0.00440	0.00545	0.00447	0.00882	0.00681		
V16	2.75	672.62	18.009	+	0.00949	0.03333	0.00900	0.00660	0.00111	0.01660	0.00000	0.00710	0.01411	0.00984	0.00232	0.02626	0.00221	0.00997	0.00287	0.02380	0.00216	0.00231	0.01773	0.00395		
V17	2.57	295.17	13.644	-	0.01638	0.00236	0.01460	0.01560	0.00446	0.01450	0.02770	0.01680	0.00584	0.02587	0.00585	0.01620	0.01174	0.01583	0.00241	0.00513	0.01320	0.00900	0.00502	0.01290		
V18	2.65	341.11	1.837	-	0.00713	0.00454	0.00603	0.00440	0.00193	0.00410	0.00598	0.00420	0.00377	0.00817	0.00492	0.03356	0.00264	0.00338	0.00384	0.00438	0.00437	0.00264	0.00277	0.00549		
V19	2.64	371.10	8.233	+	0.00044	0.00089	0.00287	0.00000	0.00019	0.00020	0.00277	0.00125	0.00046	0.00795	0.00202	0.00017	0.00043	0.00039	0.00118	0.00251	0.00146	0.00020	0.00111	0.00060		
V20	2.61	457.18	8.233	+	0.00162	0.01020	0.00226	0.00200	0.00329	0.00160	0.00210	0.00180	0.00180	0.00210	0.00180	0.00210	0.00180	0.00210	0.00180	0.00210	0.00180	0.00210	0.00180	0.00210		
V21	2.58	277.18	13.644	-	0.01285	0.01614	0.01150	0.01200	0.00304	0.01150	0.01300	0.01150	0.01300	0.00475	0.02166	0.00606	0.01350	0.00146	0.01216	0.01196	0.00404	0.01170	0.00404	0.01170		
V22	2.55	307.28	2.367	+	0.00719	0.00519	0.00450	0.00594	0.00290	0.00276	0.00865	0.00875	0.04888	0.00835	0.00957	0.05885	0.00411	0.00247	0.00314	0.01040	0.00545	0.00432	0.00681	0.00521		
V23	2.55	459.09	8.914	+	0.05034	0.08195	0.05710	0.05680	0.05690	0.04770	0.04570	0.05550	0.05880	0.04328	0.05691	0.06350	0.05310	0.04888	0.05730	0.05430	0.06330	0.06750	0.04850	0.05560		
V24	2.54	245.92	14.654	-	0.00000	0.00000	0.00000	0.00223	0.00223	0.00223	0.00223	0.00223	0.00223	0.00223	0.00223	0.00223	0.00223	0.00223	0.00223	0.00223	0.00223	0.00223	0.00223			
V25	2.39	531.64	11.073	-	0.00000	0.00000	0.00000	0.00375	0.00259	0.00678	0.00000	0.00000	0.00000	0.00000	0.00000	0.00000	0.00000	0.00000	0.00000	0.00000	0.00000	0.00000	0.00000			
V26	2.35	337.09	9.563	-	0.00773	0.00222	0.00112	0.01220	0.01410	0.00512	0.01280	0.00871	0.00512	0.01094	0.01074	0.01018	0.00918	0.00684	0.00287	0.02220	0.01600	0.01070	0.01100	0.00672		
V27	2.32	563.14	9.646	-	0.00658	0.01150	0.01110	0.00228	0.00251	0.00257	0.00286	0.01100	0.00948	0.01058	0.01241	0.01280	0.00912	0.00251	0.00146	0.00820	0.01110	0.01190	0.01639	0.00625		
V28	2.29	457.18	8.233	+	0.00007	0.00009	0.00000	0.00000	0.00000	0.00000	0.00000	0.00000	0.00000	0.00000	0.00000	0.00000	0.00000	0.00000	0.00000	0.00000	0.00000	0.00000				
V29	2.28	565.15	9.616	-	0.01701	0.02221	0.02280	0.00699	0.00889	0.00795	0.01800	0.02070	0.01978	0.02230	0.02600	0.00367	0.00681	0.00412	0.01820	0.02250	0.02070	0.02120	0.01420			
V30	2.21	424.09	8.708	-	0.00000	0.00000	0.00000	0.00193	0.00273	0.00218	0.00000	0.00000	0.00000	0.00000	0.00000	0.00000	0.00000	0.00000	0.00000	0.00000	0.00000	0.00000				
V31	2.04	391.99	10.811	-	0.00282	0.00344	0.00458	0.00118	0.00118	0.00118	0.00118	0.00118	0.00118	0.00118	0.00118	0.00118	0.00118	0.00118	0.00118	0.00118	0.00118	0.00118				
V32	2.03	158.08	2.173	+	0.00400	0.00178	0.00093	0.00480	0.00221	0.01417	0.00343	0.00294	0.00248	0.00949	0.00247	0.01048	0.00172	0.01092	0.01072	0.00488	0.00296	0.00508	0.00448	0.00255		
V33	2.01	303.05	10.143	+	0.01680	0.01634	0.02530	0.00684	0.00858	0.00981	0.01650	0.01410	0.02090	0.02098	0.01255	0.01780	0.01960	0.02113	0.02090	0.01440	0.01110	0.01750	0.00584	0.00525		
V34	1.96	524.13	11.003	-	0.00005	0.00051	0.00086	0.00304	0.00391	0.00473	0.00000	0.00000	0.00205	0.00046	0.00171	0.01128	0.00000	0.00000	0.00000	0.00000	0.00254	0.00719	0.00744			
V35	1.90	306.06	13.644	-	0.04370	0.03586	0.03586	0.00220	0.00220	0.00220	0.00220	0.00220	0.00220	0.00220	0.00220	0.00220	0.00220	0.00220	0.00220	0.00220	0.00220	0.00220				
V36	1.76	291.08	9.181	+	0.01825	0.02057	0.02290	0.02310	0.02480	0.02180	0.02210	0.02140	0.02210	0.02140	0.02177	0.01931	0.02100	0.01710	0.01330	0.02360	0.01950	0.02200	0.02810	0.02310		
V37	1.71	577.15	10.015	-	0.00079	0.00214	0.00243	0.00117	0.00196	0.00235	0.00190	0.00041	0.00158	0.00046	0.00111	0.01019	0.00094	0.00175	0.01054	0.00227	0.00039	0.00124	0.00218	0.00273		
V38	1.70	291.99	10.811	-	0.00062	0.00067	0.00091	0.00018	0.00018	0.0																

Supplementary Table S7. Selected peaks with the highest VIP values (>1) contributing to the construction of the polyphenol-predictive OPLS regression model in MALDI-MS datasets.

Variables	m/z	VIP	(Name) (Polyphenol)	AT1	AT2	AT3	BF1	BF2	BF3	KM1	KM2	KM3	SM1	SM2	SM3	SR1	SR2	SR3	YB1	YB2	YB3	YM1	YM2	YM3
V01	170.08	3.52		1.93	2.11	2.54	2.04	2.56	2.54	2.00	2.11	2.41	1.96	2.13	2.33	2.44	2.33	2.17	2.12	2.13	2.34	2.21	2.28	2.65
V02	305.19	3.20		0.04360	0.00010	0.00010	0.00010	0.00010	0.00010	0.03820	0.00010	0.00010	0.00010	0.00010	0.00010	0.00010	0.00010	0.00010	0.00010	0.00010	0.00010	0.00010	0.00010	0.00010
V03	132.97	2.69		0.04070	0.05580	0.05710	0.04220	0.05710	0.05640	0.04840	0.05490	0.06950	0.04650	0.05640	0.06680	0.03360	0.03900	0.03480	0.04070	0.04740	0.05710	0.05080	0.05760	0.07250
V04	289.19	2.33		0.02420	0.01270	0.00620	0.02820	0.01910	0.01290	0.02080	0.01800	0.00780	0.02170	0.01770	0.00530	0.01890	0.02490	0.01750	0.01740	0.02430	0.01120	0.01720	0.01440	0.00760
V05	441.14	2.32		0.01740	0.02260	0.02420	0.02320	0.02910	0.02810	0.02010	0.02240	0.02800	0.01770	0.02130	0.02640	0.01710	0.02070	0.01810	0.01880	0.02030	0.02390	0.02260	0.02430	0.03130
V06	167.02	2.16		0.02020	0.02440	0.02740	0.01770	0.03010	0.03130	0.01920	0.01950	0.02150	0.01100	0.02310	0.02360	0.01930	0.01690	0.02310	0.01690	0.02090	0.02160	0.01820	0.02850	0.02830
V07	287.18	2.08		0.03350	0.04280	0.03930	0.03170	0.04120	0.04050	0.03320	0.04130	0.04190	0.02930	0.04160	0.04250	0.03550	0.03490	0.03890	0.03260	0.04010	0.04140	0.03630	0.04240	0.04400
V08	457.20	2.02		0.01840	0.02460	0.02430	0.01870	0.02530	0.02710	0.02030	0.02370	0.02530	0.01500	0.02350	0.02690	0.02110	0.02020	0.02290	0.01930	0.02240	0.02510	0.02070	0.02610	0.02680
V09	166.02	2.01		0.04110	0.04880	0.04720	0.03150	0.04970	0.04680	0.04130	0.04830	0.04580	0.02840	0.04720	0.04750	0.04080	0.03790	0.04940	0.04040	0.04800	0.04600	0.04200	0.05490	0.05130
V10	168.06	2.00		0.02010	0.02660	0.02670	0.02160	0.02760	0.02640	0.02350	0.02720	0.03310	0.02200	0.02880	0.02880	0.01890	0.02170	0.01980	0.02080	0.02380	0.02720	0.02470	0.02700	0.03320
V11	136.99	2.00		0.03590	0.04550	0.04220	0.03360	0.04430	0.04410	0.03490	0.04430	0.04190	0.03110	0.04410	0.04750	0.04240	0.04460	0.05190	0.03490	0.04410	0.04580	0.03820	0.04430	0.04410
V12	116.99	1.99		0.01580	0.01990	0.01870	0.01580	0.02200	0.02050	0.01750	0.02100	0.02330	0.01910	0.01810	0.02760	0.01610	0.02000	0.01610	0.01560	0.02080	0.02480	0.01980	0.01940	0.02440
V13	176.01	1.88		0.00660	0.00380	0.00010	0.00800	0.00310	0.00270	0.00510	0.00510	0.00260	0.00730	0.00770	0.00010	0.00710	0.00460	0.00390	0.00510	0.00560	0.00440	0.00600	0.00390	0.00010
V14	209.19	1.82		0.00480	0.00450	0.00010	0.00470	0.00010	0.00320	0.00440	0.00460	0.00010	0.00010	0.00010	0.00010	0.00450	0.00010	0.00400	0.00440	0.00500	0.00010	0.00490	0.00410	0.00010
V15	177.14	1.79		0.00850	0.00010	0.00010	0.00960	0.00010	0.00010	0.00760	0.00010	0.00010	0.00870	0.00010	0.00010	0.00850	0.00010	0.00010	0.00750	0.00870	0.00010	0.00780	0.00010	0.00010
V16	125.02	1.74		0.00720	0.00010	0.00010	0.00700	0.00010	0.00460	0.00660	0.00010	0.00010	0.00910	0.00010	0.00010	0.00740	0.00730	0.00640	0.00630	0.00010	0.00010	0.00740	0.00010	0.00010
V17	288.20	1.74		0.01650	0.02010	0.01800	0.01510	0.02120	0.02050	0.01570	0.01890	0.01940	0.01560	0.01750	0.02650	0.01800	0.01860	0.01840	0.01550	0.02150	0.02410	0.01780	0.01940	0.02110
V18	204.14	1.72		0.00940	0.01320	0.01380	0.00970	0.01400	0.01560	0.01010	0.01220	0.01400	0.00730	0.01250	0.01640	0.01010	0.01000	0.01210	0.00960	0.01130	0.01330	0.01040	0.01390	0.01460
V19	144.99	1.50		0.01590	0.00010	0.00010	0.00010	0.00010	0.00010	0.00010	0.00010	0.00010	0.00010	0.00010	0.00010	0.00010	0.00010	0.00010	0.00010	0.01970	0.00010	0.00010	0.02430	0.00010
V20	162.64	1.49		0.00010	0.00580	0.00530	0.00010	0.00590	0.00580	0.00010	0.00580	0.00560	0.00010	0.00580	0.00570	0.00010	0.00010	0.00580	0.00550	0.00010	0.00590	0.00630	0.00610	0.00600
V21	138.00	1.48		0.00920	0.01210	0.01130	0.00930	0.01290	0.01240	0.01030	0.01230	0.01350	0.01050	0.01100	0.01690	0.00840	0.01020	0.00870	0.00900	0.01190	0.01440	0.01110	0.01150	0.01440
V22	755.31	1.46		0.01170	0.01220	0.01200	0.00370	0.00640	0.00490	0.01450	0.01310	0.00850	0.01030	0.01520	0.00970	0.00010	0.00010	0.00010	0.01500	0.01350	0.00850	0.00920	0.00850	0.00430
V23	128.00	1.45		0.00430	0.00180	0.00010	0.01670	0.00640	0.00240	0.00740	0.00610	0.00010	0.01520	0.00340	0.00010	0.00530	0.00610	0.00370	0.00930	0.00550	0.00210	0.01210	0.00300	0.00240
V24	175.44	1.34		0.00200	0.00190	0.00170	0.01280	0.00010	0.00190	0.00180	0.00190	0.00170	0.01810	0.00010	0.00220	0.00010	0.00010	0.00010	0.00200	0.00200	0.00210	0.00230	0.00210	0.00010
V25	307.24	1.34		0.00440	0.00530	0.00500	0.00400	0.00010	0.00010	0.00490	0.00510	0.00010	0.00430	0.00010	0.00010	0.00390	0.00400	0.00370	0.00440	0.00490	0.00520	0.00510	0.00510	0.00010
V26	145.99	1.25		0.01070	0.00620	0.00510	0.01140	0.00740	0.00520	0.01190	0.01000	0.00710	0.01500	0.00810	0.00360	0.00960	0.00810	0.00630	0.01150	0.01060	0.00860	0.01290	0.00910	0.00760
V27	293.20	1.24		0.00010	0.00010	0.00260	0.00010	0.00010	0.00290	0.00010	0.00010	0.00010	0.00010	0.00010	0.00010	0.00010	0.00010	0.00010	0.00010	0.00010	0.00010	0.00010	0.00320	0.00340
V28	126.97	1.23		0.00850	0.00430	0.00010	0.00680	0.00510	0.00010	0.00660	0.00450	0.00010	0.00720	0.00360	0.00400	0.00650	0.00700	0.00380	0.00610	0.00690	0.00470	0.00730	0.00380	0.00400
V29	756.29	1.23		0.00410	0.00440	0.00440	0.00010	0.00010	0.00010	0.00530	0.00470	0.00290	0.00010	0.00550	0.00350	0.00010	0.00010	0.00010	0.00560	0.00480	0.00260	0.00310	0.00010	0.00010
V30	456.09	1.20		0.01440	0.01790	0.01790	0.01090	0.01810	0.01750	0.01540	0.01820	0.01610	0.00970	0.01720	0.01640	0.01380	0.01220	0.01770	0.01460	0.01730	0.01630	0.01450	0.02140	0.01900
V31	202.14	1.17		0.00740	0.00010	0.00010	0.00010	0.00010	0.00010	0.00010	0.00010	0.00010	0.00010	0.00010	0.00010	0.00010	0.00010	0.00010	0.00640	0.00010	0.00010	0.00010	0.00010	0.00010
V32	160.13	1.15		0.00960	0.00700	0.00420	0.00720	0.00630	0.00440	0.00770	0.00780	0.00500	0.00970	0.00690	0.00010	0.01030	0.00010	0.00530	0.00970	0.00900	0.00570	0.00990	0.00710	0.00560
V33	124.01	1.15		0.00800	0.01020	0.00890	0.00730	0.00960	0.00970	0.00710	0.00880	0.00920	0.00710	0.00850	0.01310	0.00810	0.00790	0.00830	0.00730	0.01050	0.01210	0.00800	0.00970	0.01040
V34	479.57	1.14		0.00830	0.01010	0.02060	0.00010	0.00010	0.00910	0.00880	0.00010	0.01390	0.00010	0.01020	0.01940	0.03020	0.02440	0.03290	0.00770	0.00010	0.01480	0.00010	0.00760	0.00860
V35	220.15	1.10		0.00340	0.00010	0.00010	0.00010	0.00010	0.00010	0.00250	0.00010	0.00010	0.00010	0.00010	0.00010	0.00010	0.00010	0.00010	0.00260	0.00010	0.00010	0.00010	0.00010	0.00010
V36	304.16	1.06		0.00720	0.00970	0.00970	0.00680	0.00890	0.00980	0.00810	0.00910	0.01010	0.00890	0.00890	0.01010	0.00660	0.00640	0.00680	0.00730	0.00790	0.00860	0.00810	0.00970	0.01070
V37	286.15	1.02		0.00710	0.00920	0.01010	0.00600	0.00820	0.00930	0.00850	0.00910	0.00980	0.00640	0.00970	0.01060	0.00940	0.00840	0.00920	0.00800	0.00800	0.00910	0.00770	0.00980	0.00920
V38	354.53	1.01		0.00190	0.00010	0.00010	0.00140	0.00010	0.00010	0.00170	0.00010	0.00010	0.00010	0.00010	0.00010	0.00010	0.00010	0.00010	0.00180	0.00010	0.00010	0.00200	0.00010	0.00010